*Int. J. Heat Mass Transfer.* Vol. 30, No. 11, pp. 2433–2440, 1987
Printed in Great Britain

0017–9310/87 $3.00 + 0.00


# Natural convection in rectangular enclosures heated from below and cooled along one side

M. NOVEMBER and M. W. NANSTEEL
Department of Mechanical Engineering and Applied Mechanics, University of Pennsylvania, Philadelphia, PA 19104, U.S.A.

(*Received* 23 *January* 1987 *and in final form* 27 *April* 1987)

**Abstract**—Steady natural convection in a square, water-filled enclosure heated from below and cooled on one vertical side is studied analytically and numerically. Expansions for small Rayleigh number are developed to order $Ra^2$. It is found that the first contribution to the convective heat transfer occurs at order $Ra^2$. Asymptotic expressions are found for the temperature and heat transfer near the flux singularity on the enclosure floor. Finite difference numerical simulations indicate that the present condition (heating from below) is quite distinct from the case of cooling from below and heating on one vertical wall. Convective heat transfer is shown to be most significant when slightly less than half of the lower surface is heated.

## 1. INTRODUCTION

NATURAL convection in fluid-filled rectangular enclosures has received considerable attention over the past several years. This attention is due in part to the wide variety of important applications that involve natural convection processes. These applications span such diverse fields as solar energy collection; nuclear reactor operation and safety; the energy efficient design of buildings, rooms, and machinery; waste disposal; and fire prevention and safety.

Most of the previous work has addressed natural convection in rectangular geometries due to either a vertically or horizontally imposed heat flux or temperature difference. Rather little work has been carried out for more complex boundary conditions such as the case when the imposed gradient is neither horizontal nor vertical. Kimura and Bejan [1] considered natural convection in a rectangular enclosure with the entire lower surface cooled while one vertical wall was heated. Constant heat flux as well as isothermal boundary conditions were considered. Small Rayleigh number expansions indicated [1] that qualitative features of the $Ra \to 0$ flow are relatively insensitive to the nature of the boundary condition. Numerical simulations carried out for the isothermal case indicated [1] a single-cell flow, the center of which draws nearer and nearer to the singular corner (where temperature is discontinuous) with increasing Rayleigh number. In all cases the enclosed fluid remained stably stratified. Anderson and Lauriat [2] studied the flow in a square enclosure with a uniform flux or isothermal (heating) condition on the lower surface while one vertical wall was cooled isothermally. Numerical calculations [2] for flux Raylcigh numbers in the range $10^6$–$10^{10}$ indicated a single cell flow with a stable boundary layer adjacent to the heated floor. Experimental observations [2] confirmed the absence of Bénard-type instabilities for flux Rayleigh numbers as large as $5 \times 10^{13}$. Torrance and Rockett [3] numerically studied the convection of air in a vertical cylindrical enclosure which was cooled on the boundary except for a small hot spot centered on the lower surface. Torrance *et al.* [4] investigated convection in this geometry experimentally while a similar problem was studied numerically by Greenspan and Shultz [5]. In ref. [3] it was found that for a Grashof number less than $4 \times 10^9$ the flow consisted of a single, steady toroidal roll with upflow near the axis of the cylinder. For Grashof numbers greater than about $10^6$ the flow was dominated by a rising column of hot fluid near the vertical axis of the cylinder just above the hot spot. The center of the toroidal cell moved toward the upper outside corner of the cylinder as Grashof number was increased. For Grashof numbers exceeding $4 \times 10^6$, a large thermally stratified region developed and occupied most of the enclosure interior. Finite heat transfer rates were obtained in ref. [3] by assuming a ramp temperature change at the edge of the hot spot. Chao *et al.* [6] experimentally and numerically investigated natural convection in an inclined box with the lower surface half-heated and half-insulated and the upper surface cooled. It was found [6] that a single pair of rolls developed when half of the lower surface was heated. It was also shown that partial heating of the lower surface resulted in convective motion for all Rayleigh numbers ($>0$). Shiralkar and Tien [7] carried out a numerical investigation of convection in a rectangular enclosure due to temperature gradients imposed in the horizontal and vertical directions simultaneously. It was found [7] that a strong stabilizing vertical temperature gradient resulted in lower vertical velocities and the generation of secondary vortices at opposite corners of the enclosure. For strong destabilizing vertical gradients, the stable stratification in the enclosure core was destroyed and unstably stratified thermal layers formed adjacent to the upper and lower surfaces of

## NOMENCLATURE

| | |
|---|---|
| $g$ | gravitational acceleration |
| $h$ | mesh spacing |
| $\mathbf{j}$ | unit vector in vertical direction |
| $k$ | thermal conductivity |
| $l$ | length of unheated section |
| $L$ | enclosure width |
| $n$ | normal coordinate |
| $Nu$ | Nusselt number, $Q(1)/Q(1)_{\text{cond}}$ |
| $Nu_i$ | coefficient in expansion (23) |
| $p$ | dimensionless pressure, $(\bar{p}+\rho_c g\bar{y})L^2/\rho_c v_c^2$ |
| $\bar{p}$ | pressure |
| $Pr$ | Prandtl number, $v_c/\alpha_c$ |
| $q_i$ | coefficient given by equation (22) |
| $q''(x)$ | horizontal energy flux averaged over vertical cross section |
| $Q(x)$ | dimensionless horizontal heat transfer rate, equation (7) |
| $r$ | radial coordinate |
| $Ra$ | Rayleigh number, $g\beta(\bar{T}_h-\bar{T}_c)L^3/v_c\alpha_c$ |
| $t$ | dimensionless time, $\bar{t}v_c/L^2$ |
| $\bar{t}$ | time |
| $T$ | dimensionless temperature, $(\bar{T}-\bar{T}_c)/(\bar{T}_h-\bar{T}_c)$ |
| $\bar{T}$ | temperature |
| $T_i$ | coefficient in expansion (13) |
| $u$ | dimensionless horizontal component of velocity, $\bar{u}L/v_c$ |
| $\bar{u}$ | horizontal component of velocity |
| $\mathbf{u}$ | dimensionless velocity, $\bar{\mathbf{u}}L/v_c$ |
| $\bar{\mathbf{u}}$ | velocity |
| $v$ | dimensionless vertical component of velocity, $\bar{v}L/v_c$ |
| $\bar{v}$ | vertical component of velocity |
| $x$ | dimensionless horizontal coordinate, $\bar{x}/L$ |
| $\bar{x}$ | horizontal coordinate |
| $y$ | dimensionless vertical coordinate, $\bar{y}/L$ |
| $\bar{y}$ | vertical coordinate. |

Greek symbols

| | |
|---|---|
| $\alpha$ | thermal diffusivity |
| $\beta$ | coefficient of thermal expansion |
| $\varepsilon$ | dimensionless length of unheated section, $l/L$ |
| $\theta$ | angular coordinate |
| $\nu$ | kinematic viscosity |
| $\rho$ | density |
| $\psi$ | dimensionless streamfunction, $\bar{\psi}/v_c$ |
| $\bar{\psi}$ | streamfunction |
| $\psi_i$ | coefficient in expansion (11) |
| $\omega$ | dimensionless vorticity, $\bar{\omega}L^2/v_c$ |
| $\bar{\omega}$ | vorticity |
| $\omega_i$ | coefficient in expansion (12). |

Subscripts

| | |
|---|---|
| c | cold wall |
| cond | pure conduction |
| h | hot surface. |

the enclosure. Poulikakos [8] examined the convection in an enclosure with heated and cooled regions on a single vertical wall. It was noted [8] that convective patterns differed markedly depending on whether the heated section was above or below the cooled section of the boundary. When the lower portion of the vertical surface was heated, convective motion was more intense and thermal penetration was more complete than when the upper portion of the surface was heated.

The objective of the present study is to clearly understand the heat transfer mechanisms present when a portion of the lower surface of a water-filled rectangular enclosure is heated while one of the vertical walls is cooled. Special attention will be given to the effects of heating intensity (Rayleigh number) and the length of the heated segment on the resulting flow structure, temperature field and heat transfer. Comparisons with the findings of ref. [1] (heating on one side and cooling from below) will be made.

## 2. FORMULATION

Consider the square, fluid-filled enclosure, Fig. 1, in which the lower surface is heated ($\bar{T} = \bar{T}_h$) over the segment $0 < \bar{x} < L-l$ while the right-hand wall is maintained at $\bar{T} = \bar{T}_c < \bar{T}_h$. The remaining portion of the boundary is thermally insulated. Assuming that the temperature difference $(\bar{T}_h-\bar{T}_c)$ is small so that the Boussinesq assumption is valid and that fluid motions are confined to the plane of Fig. 1, the time-

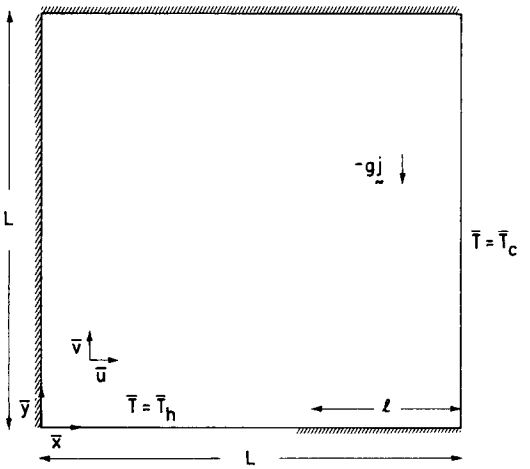


FIG. 1. Square enclosure with heating from below and cooling on one side.

dependent equations of mass, momentum and energy conservation in dimensionless form are

$$\operatorname{div}\mathbf{u} = 0 \tag{1}$$

$$\frac{\mathrm{D}\mathbf{u}}{\mathrm{D}t} = -\nabla p + \frac{Ra}{Pr} T\mathbf{j} + \nabla^2\mathbf{u} \tag{2}$$

$$\frac{\mathrm{D}T}{\mathrm{D}t} = \frac{1}{Pr}\nabla^2 T \tag{3}$$

where

$$p = (\bar{p} + \rho_c g\bar{y})L^2/\rho_c v_c^2$$

$$T = (\bar{T} - \bar{T}_c)/(\bar{T}_h - \bar{T}_c)$$

and distance, velocity and time have been made dimensionless with the quantities $L$, $v_c/L$ and $L^2/v_c$. Conditions on the boundary are

$$\mathbf{u} = 0$$

$$T(1, y) = \frac{\partial T}{\partial y}(x, 1) = \frac{\partial T}{\partial x}(0, y) = 0$$

$$T(x, 0) = 1, \quad x \leqslant 1-\varepsilon$$

$$\frac{\partial T}{\partial y}(x, 0) = 0, \quad x > 1-\varepsilon$$

where $\varepsilon = l/L$. Note that on the lower boundary $x = 1-\varepsilon$ is a point of flux singularity [9, 10]. Eliminating $p$ from equation (2) and introducing the streamfunction $\psi$, and vorticity $\omega$

$$u = \frac{\partial\psi}{\partial y}, \quad v = -\frac{\partial\psi}{\partial x}, \quad \omega = -\nabla^2\psi \tag{4}$$

yields

$$\frac{\partial\omega}{\partial t} + \frac{\partial\psi}{\partial y}\frac{\partial\omega}{\partial x} - \frac{\partial\psi}{\partial x}\frac{\partial\omega}{\partial y} = \nabla^2\omega + \frac{Ra}{Pr}\frac{\partial T}{\partial x} \tag{5}$$

$$\frac{\partial T}{\partial t} + \frac{\partial\psi}{\partial y}\frac{\partial T}{\partial x} - \frac{\partial\psi}{\partial x}\frac{\partial T}{\partial y} = \frac{1}{Pr}\nabla^2 T \tag{6}$$

with

$$\psi = \frac{\partial\psi}{\partial n} = 0, \quad \text{on the boundary.}$$

The non-dimensional rate of energy transfer across any vertical plane is

$$Q(x) = \frac{q''(x)L}{k(\bar{T}_h - \bar{T}_c)} = \int_0^1 \left(Pr\, Tu - \frac{\partial T}{\partial x}\right)\mathrm{d}y. \tag{7}$$

Note that under steady conditions $Q(x)$ = constant for $x > 1-\varepsilon$. The corresponding Nusselt number is

$$Nu = Q(1)/Q(1)_{\text{cond}}. \tag{8}$$

## 3. HEAT TRANSFER NEAR THE FLUX SINGULARITY

In the neighborhood of the mixed boundary point ($y = 0$, $x = 1-\varepsilon$) energy transport in the fluid is dominated by conduction because of the no-slip condition. Hence the temperature field asymptotically near the singularity will be that due to conduction only. This can be shown by considering a system of polar $(r, \theta)$ coordinates (centered at the flux singularity with $\theta = 0$ on the adiabatic surface) and substituting the asymptotic forms

$$\left.\begin{aligned} \psi &\sim r^\gamma f(\theta), \quad \gamma \geqslant 1 \\ T &\sim 1 + r^\eta g(\theta), \quad \eta \geqslant 0 \end{aligned}\right\} r \to 0$$

into the steady form of equations (4)–(6). This results in a pair of eigenvalue problems [11] for the functions $g(\theta)$ and $f(\theta)$. It follows [11] that the limiting ($r \to 0$) behaviors are

$$\left.\begin{aligned} \psi &\sim C_1 r^2 \sin^2\theta \\ T &\sim 1 + C_2 r^{1/2}\cos(\theta/2) \end{aligned}\right\} r \to 0 \tag{9}$$

where $C_1$ and $C_2$ are constants which are determined by conditions imposed in the far field. The first equation of equations (9) corresponds to a flow parallel to the wall, while the second is identical to the relation found in ref. [10] for the asymptotic behavior in a solid. It follows that the heat flux through the lower boundary near the singularity is of the order of $r^{-1/2}$, i.e.

$$-\frac{k}{r}\frac{\partial T}{\partial\theta}(r, \pi) \sim \frac{k}{2} C_2 r^{-1/2}, \quad r \to 0. \tag{10}$$

However, the total, integrated heat transfer at the surface between the singularity and some location $r$, on $\theta = \pi$, is bounded and is of the order of $r^{1/2}$. Hence, although total energy flow is bounded the local flux is not and hence great care must be exercised near the singularity in numerical simulations [9].

## 4. SMALL RAYLEIGH NUMBER CALCULATIONS

It is assumed that $\psi$, $\omega$ and $T$ can be expanded in integral powers of $Ra$, hence

$$\psi = \psi_1\, Ra + \psi_2\, Ra^2 + \cdots \tag{11}$$

$$\omega = \omega_1\, Ra + \omega_2\, Ra^2 + \cdots \tag{12}$$

$$T = T_0 + T_1\, Ra + \cdots \tag{13}$$

Substitution of these expansions in the steady forms of equations (4)–(6) results in the following systems for the functions $\psi_i$, $\omega_i$ and $T_i$:

$$\nabla^2 T_0 = 0 \tag{14}$$

$$\nabla^2\omega_1 = -\frac{1}{Pr}\frac{\partial T_0}{\partial x} \tag{15}$$

$$\nabla^2\psi_1 = -\omega_1 \tag{16}$$

$$\nabla^2 T_1 = Pr\left(\frac{\partial\psi_1}{\partial y}\frac{\partial T_0}{\partial x} - \frac{\partial\psi_1}{\partial x}\frac{\partial T_0}{\partial y}\right) \tag{17}$$

$$\nabla^2\omega_2 = -\frac{1}{Pr}\frac{\partial T_1}{\partial x} + \frac{\partial\psi_1}{\partial y}\frac{\partial\omega_1}{\partial x} - \frac{\partial\psi_1}{\partial x}\frac{\partial\omega_1}{\partial y} \tag{18}$$

Table 1. Variation of the maximum values of $\psi_1$, $\psi_2$, $T_1$ and $T_2$ with mesh size, $\varepsilon = 1/3$

| Mesh | $(\psi_1)_{max} \times 10^4$ | $(\psi_2)_{max} \times 10^8$ | $(T_1)_{max} \times 10^4$ | $(T_2)_{max} \times 10^8$ |
|---|---|---|---|---|
| $13 \times 13$ | 1.29 | 3.13 | 1.29 | 3.62 |
| $25 \times 25$ | 1.24 | 3.03 | 1.29 | 3.74 |
| $43 \times 43$ | 1.23 | 3.02 | 1.29 | 3.76 |
| $61 \times 61$ | 1.23 | 3.02 | 1.29 | 3.77 |

$$\nabla^2 \psi_2 = -\omega_2 \tag{19}$$

$$\nabla^2 T_2 = Pr\left(\frac{\partial \psi_1}{\partial y}\frac{\partial T_1}{\partial x} - \frac{\partial \psi_1}{\partial x}\frac{\partial T_1}{\partial y} + \frac{\partial \psi_2}{\partial y}\frac{\partial T_0}{\partial x} - \frac{\partial \psi_2}{\partial x}\frac{\partial T_0}{\partial y}\right) \tag{20}$$

The corresponding conditions on the boundary are

$$\psi_i = \frac{\partial \psi_i}{\partial n} = 0, \quad i \geqslant 1$$

$$\frac{\partial T_i}{\partial x}(0, y) = \frac{\partial T_i}{\partial y}(x, 1) = 0, \quad i \geqslant 0$$

$$T_0(x, 0) = 1, \quad x < 1-\varepsilon$$

$$T_i(x, 0) = 0, \quad x > 1-\varepsilon, \quad i \geqslant 1$$

$$\frac{\partial T_i}{\partial y}(x, 0) = 0, \quad x > 1-\varepsilon, \quad i \geqslant 0.$$

From equations (7) and (13) the heat transfer at the cold wall becomes

$$Q(1) = q_0 + q_1 Ra + q_2 Ra^2 + \tag{21}$$

where

$$q_i = -\int_0^1 \frac{\partial T_i}{\partial x}(1, y)\,dy, \quad i \geqslant 0. \tag{22}$$

Note from equations (14) and (22) that the leading term, $q_0$, represents the heat transfer due to pure conduction. Hence the Nusselt number

$$Nu = 1 + Nu_1 Ra + Nu_2 Ra^2 + \cdots \tag{23}$$

where

$$Nu_i = q_i/q_0, \quad i \geqslant 1.$$

Terms in expansions (11)–(13) were calculated to order $Ra^2$ by a second-order accurate finite difference technique in conjunction with a uniform $61 \times 61$ mesh. Various criteria were used to test for convergence with mesh size, some of which are shown in Table 1. Note also that

$$\int_0^{1-\varepsilon} \frac{\partial T_i}{\partial y}(x, 0)\,dx = \int_0^1 \frac{\partial T_i}{\partial x}(1, y)\,dy, \quad i \geqslant 0.$$

This criterion, however, is not useful for evaluating convergence of the numerical scheme due to the presence of the flux singularity ($x = 1-\varepsilon$, $y = 0$) at each order. That is, large errors are incurred when attempting to numerically integrate heat flux in the neighborhood of this point. Fortunately, however, the influence of the singularity does not penetrate very far into the solution domain so that some distance away from the singularity the solution is not affected [12].

Contours of the functions $T_0$, $\psi_1$ and $T_1$ are shown in Fig. 2 for the case $\varepsilon = 1/2$.† Note that, to lowest order, flow in the enclosure consists of a single clockwise cell in which cool fluid descends along the cold wall and is swept along the lower surface of the enclosure where it is rapidly heated in the vicinity of the flux singularity, equation (10). This warmer fluid then rises adjacent to the unheated left-hand vertical wall of the enclosure. Note that the flow symmetry present at this order for the classical rectangular enclosure with a horizontally imposed temperature gradient [13] does not exist here. The cell is skewed somewhat toward the lower right quadrant of the enclosure. Qualitative

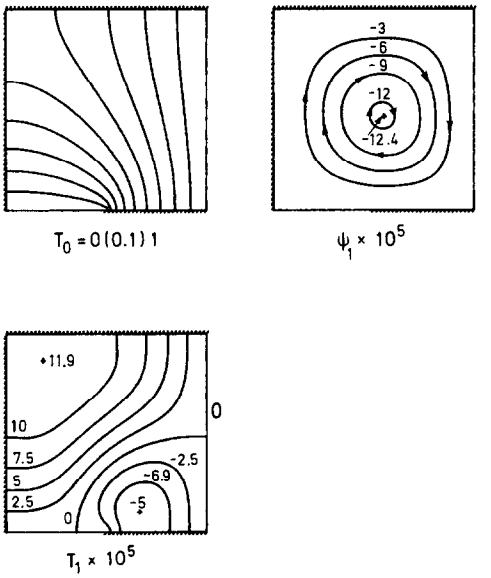


FIG. 2. Contours for $\varepsilon = 1/2$.

†In Figs. 2, 4 and 5 the notation $T = 0(0.1)1$ indicates that contours of $T$ are plotted for nine equally spaced values of $T$ between zero and unity.

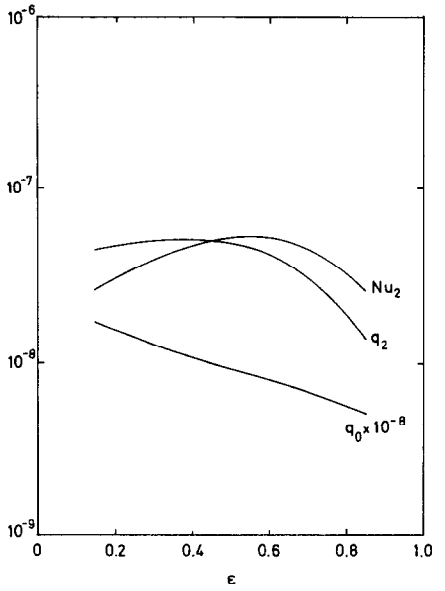


FIG. 3. Variation of $q_0$, $q_2$ and $Nu_2$ with $\varepsilon$.

features of the flow pattern changed little with changing $\varepsilon$ while circulation intensity peaked slightly near $\varepsilon = 1/2$. This behavior is reasonable since the $\varepsilon = 1$ case results in no convection ($T \equiv 0$) and in the $\varepsilon = 0$ case isotherms emerge radially from $x = 1, y = 0$ [14]. For $\varepsilon > 0$ isotherms above the insulated section tend to be more nearly vertical (i.e. parallel to the gravity vector) so that there is a greater potential for density differences to cause convective motion than in the $\varepsilon = 0$ case. The flow field shown in Fig. 2 ($\psi_1$) gives rise to the temperature perturbation ($T_1$). Note that the clockwise motion convects cool fluid along the cold wall and down into the lower right-hand quadrant of the enclosure resulting in a negative temperature perturbation there. At the same time, warm fluid adjacent to the hot surface is convected upward where it appears as a positive perturbation in the upper portion of the enclosure.

From the numerical computations it was concluded that the first correction to the conduction temperature field, $T_1$, does not contribute to the convective enhancement of the heat transfer, i.e. $q_1 = 0$. Increasingly fine mesh discretization indicated that $q_1 \propto h^2$ for mesh spacing $h \to 0$. Hence it is assumed that the very small, numerically obtained values of $q_1$ are due to discretization error in the second-order accurate scheme used here (hence the quadratic dependence on $h$). This result ($q_1 = 0$) is easily demonstrated in the case of an enclosure with differential heating in the horizontal direction [13, 15]. Figure 3 shows the conduction component $q_0$ as well as the first correction to the heat transfer due to convection $q_2$ (and $Nu_2$) as a function of $\varepsilon$. Note that conduction increases without bound as $\varepsilon \to 0$ since then, the heated and cooled surfaces are in direct contact [14]. Also, the convective enhancement of the heat transfer $Nu_2 = q_2/q_0$ is seen to be largest for $\varepsilon \simeq 0.6$ where circulation

Table 2. Variation of horizontal energy flux $Q(x)$ and maximum streamfunction with mesh size, $Ra = 10^5$, $\varepsilon = 2/3$

| Mesh | $Q(2/3)$ | $Q(1)$ | $\psi_{max}$ |
|---|---|---|---|
| $31 \times 31$ | 2.86 | 2.98 | −2.16 |
| $43 \times 43$ | 2.81 | 2.86 | −2.14 |
| $61 \times 61$ | 2.78 | 2.80 | −2.13 |

was also a maximum. By comparison with the full numerical solutions, to be discussed below, expansion (23) (to order $Ra^2$) is found to be quite accurate for $Ra \leqslant O(10^3)$.

## 5. RESULTS FOR MODERATE VALUES OF RAYLEIGH NUMBER

Equations (4)–(6) were solved by a false transient finite difference technique. The alternating direction implicit method in conjunction with central differencing was used in almost all cases. For $Ra = 10^6$ and $\varepsilon = 1/6$ upwind differencing of convective derivatives was found to be necessary in order to obtain a stable solution. Calculations were made on increasingly fine meshes until the horizontal energy flux, equation (7), across two vertical sections of the enclosure ($x > 1-\varepsilon$) differed by less than 5% for a given mesh and the maximum value of the streamfunction changed by less than 1% with mesh size (Table 2). A uniform $61 \times 61$ mesh was the finest used.

Figure 4 shows contours of $T$ and $\psi$ for the enclos-

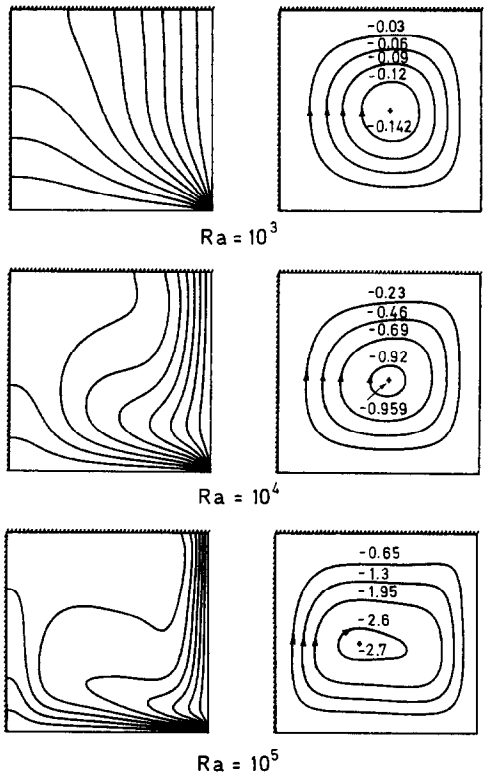


FIG. 4. Contours for $\varepsilon = 0$; $T = 0(0.1)1$, $\psi$.

ure with the entire lower surface heated, $\varepsilon = 0$. In each case ($Ra = 10^3, 10^4, 10^5$) isotherms emerge radially from the lower right-hand corner of the enclosure where heat flux on both the vertical and horizontal surfaces is unbounded [14]. For small $Ra$ ($=10^3$) the temperature distribution deviates only slightly from the diagonally symmetric conduction distribution observed for $Ra = 0$. The weak clockwise recirculation tends to lift warmer fluid away from the hot surface ($x \leqslant 1/2$) and into the upper portion of the enclosure. This results in a spreading of the isotherms in the lower left quadrant of the enclosure and compression in the upper right quadrant. As the recirculation intensity increases, $Ra = 10^4$, warm fluid is swept vertically upward along the left-hand adiabatic surface and then horizontally toward the upper section of the cold wall. This fluid is then cooled as it flows vertically downward along the cold wall. At a Rayleigh number of $10^5$ circulation has increased to a degree such that distinct thermal boundary layers can be observed adjacent to the heated and cooled surfaces. Note that the heated layer adjacent to the lower surface remains attached up to the turning corner $x = y = 0$ though the density stratification in this layer is unstable. This observation agrees with the result of Anderson and Lauriat [2] in the case of a uniform flux boundary condition on the lower surface. It is not certain whether this layer would remain attached for smaller aspect ratio enclosures or significantly larger values of $Ra$. It is also observed that the central portion of the enclosure tends to become relatively inactive with little variation in temperature as $Ra$ increases. The behavior found here is quite distinct from the behavior noted by Kimura and Bejan [1] for the case of cooling from below and heating on one vertical wall. For these thermal conditions cool fluid is swept along the lower surface and into the singular corner $x = 1, y = 0$ before rising adjacent to the heated vertical boundary. In ref. [1] the location of the streamfunction maximum moved toward the singular corner with increasing $Ra$ and the fluid remained stably stratified throughout the enclosure. When cooling from below the intensity of circulation is much less than that found for the present boundary conditions. It seems that the convective cell observed in ref. [1] is somewhat confined to the singular corner region while in the present case convective effects are more uniformly distributed over the entire outer periphery of the enclosure.

In Fig. 5 contours of $T$ and $\psi$ are shown for various insulation lengths $\varepsilon$ and $Ra = 10^6$. Comparison with Fig. 4 indicates that with the increase in $Ra$, thermal and hydrodynamic boundary layers have become more distinct and a small secondary cell has formed within the main cell near the cold wall. The appearance of secondary vortices at large $Ra$ in the core of differentially heated enclosures was attributed to a sign change in the horizontal core temperature gradient by Mallinson and de Vahl Davis [16]. It is thought that a similar mechanism may be in effect here since

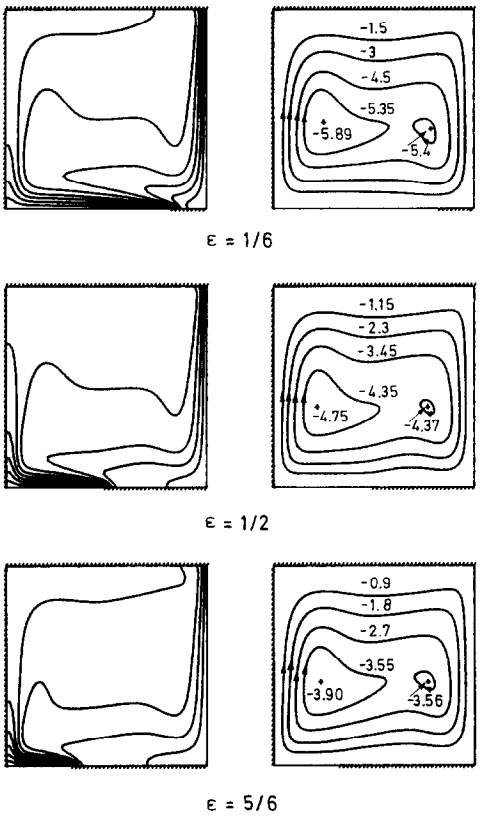


FIG. 5. Contours for $Ra = 10^6$; $T = 0(0.1)1$, $\psi$.

$\partial T/\partial x$ does take on positive values at some locations in the core for $Ra \gtrsim 10^5$. Also, Fig. 5 indicates that convection intensity decreases slowly and monotonically with increasing $\varepsilon$ ($1/6 \leqslant \varepsilon \leqslant 5/6$) in contrast to the behavior noted at small $Ra$. However, this is not surprising since the flow structure arises as a consequence of the temperature field which is highly distorted for $Ra \gtrsim O(10^4)$. Note that as the insulated section increases in length, $\varepsilon \to 1$, the velocity and temperature fields approach the limiting, stagnant condition $\mathbf{u} = T \equiv 0$. For $\varepsilon = 5/6$ most of the fluid in the enclosure is weakly but stably stratified.

Figure 6 shows the variation of dimensionless heat transfer rate $Q(1) = Q_c$ with $\varepsilon$ for $0 \leqslant Ra \leqslant 10^6$. It is observed that for each value of $Ra$ heat transfer falls rather sharply to zero as $\varepsilon$ approaches unity. This is because the heat flux in the neighborhood of the mixed boundary condition ($x \leqslant 1-\varepsilon$) is quite large (see equation (10)). Hence significant rates of heat transfer result even when only a small fraction of the lower boundary is heated. In this regime, $\varepsilon \to 1$, conduction heat transfer is dominant. It is demonstrated in ref. [10] that over 10% of the total heat transfer from a surface may occur over only 1% of the surface area adjacent to a flux singularity of the type encountered here. Note that for small values of $Ra$ ($\lesssim 10^4$), Fig. 6, heat transfer increases slowly with decreasing $\varepsilon$ (away from $\varepsilon = 1$ and 0). However, for larger $Ra$ ($\gtrsim 10^5$) heat transfer increases quite sharply

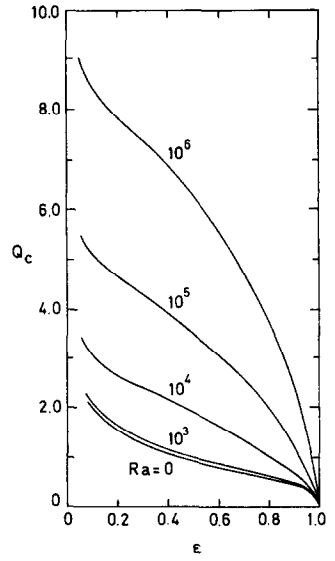


FIG. 6. Heat transfer variation with ε.

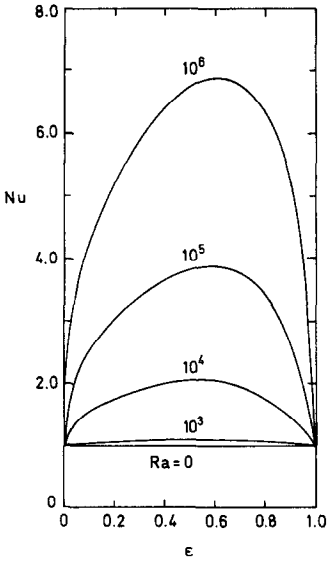


FIG. 7. Nusselt number variation with ε.

over the full range of ε. This is because for high Rayleigh numbers the strong convection sweeps cool fluid over the entire length of the heated section on the lower boundary so that a rather high rate of heat transfer exists even far downstream of the flux singularity (see also Fig. 4). For values of ε approaching zero the dominant mode of heat transfer is again conduction as most of the energy transfer (tending toward infinity as $\varepsilon \to 0$) occurs in the neighborhood of the lower right-hand corner of the enclosure. As $\varepsilon \to 0$ the flux singularity degenerates into a singularity of higher order for which the flux is non-integrable [14]. Figure 7 shows Nusselt number as a function of ε. Since *Nu* here is a relative measure of the total heat transfer with respect to the heat transfer due purely to conduction, equation (8), *Nu* tends to unity for $\varepsilon \to 0, 1$. Note also that the curves in Fig. 7 exhibit a maximum near $\varepsilon = 0.6$. Hence energy transport by convection is most significant when slightly less than one-half of the lower boundary is heated.

## 6. CONCLUSIONS

Steady natural convection in a water-filled square enclosure with one vertical wall cooled and partial heating of the lower surface has been studied. The conduction dominated behavior near the mixed boundary point was shown to consist of a parallel shear flow and heat flux of the order of $r^{-1/2}$. Expansions of streamfunction and temperature for small values of the Rayleigh number were obtained to order $Ra^2$. It was shown that the first correction to the Nusselt number for convective effects occurred at order $Ra^2$ and was largest near $\varepsilon = 0.6$. Finite difference solutions to the full equations of motion were obtained for $0 \leqslant Ra \leqslant 10^6$ and several values of ε in the range $0 \leqslant \varepsilon \leqslant 1$. The flow structure was found to consist of a single clockwise cell with strong thermal boundary layers adjacent to the heated and cooled surfaces for $Ra \gtrsim O(10^5)$. The heated layer on the lower surface remained attached over the entire horizontal span of the enclosure in all cases. The flow structure and temperature field in the present study differed dramatically from the behavior reported by Kimura and Bejan [1] in which the enclosed fluid was cooled from below ($\varepsilon = 0$) and heated along one vertical side. Also it was found that rather high rates of heat transfer persist even when a substantial portion of the lower surface is insulated. Nusselt number was shown to reach a maximum when the insulation spans slightly more than half of the lower surface.

*Acknowledgement*—The authors are grateful for the support of the National Science Foundation under Grant Nos. MEA 83-15337 and MEA 14322. The authors also wish to thank Professor B. Gebhart for his many helpful comments with regard to this work.

## REFERENCES

1. S. Kimura and A. Bejan, Natural convection in a differentially heated corner region, *Physics Fluids* **28,** 2980–2989 (1985).
2. R. Anderson and G. Lauriat, The horizontal natural convection boundary layer regime in a closed cavity, *Proc. 8th Int. Heat Transfer Conf.*, San Francisco, California, pp. 1453–1458 (1986).
3. K. Torrance and J. Rockett, Numerical study of natural convection in an enclosure with localized heating from below—creeping flow to the onset of laminar instability, *J. Fluid Mech.* **36,** 33–54 (1969).
4. K. E. Torrance, L. Orloff and J. A. Rockett, Experiments on natural convection in enclosures with localized heating from below, *J. Fluid Mech.* **36,** 21–31 (1969).
5. D. Greenspan and D. Shultz, Natural convection in an

enclosure with localized heating from below, *Comput. Meth. Appl. Mech. Engng* **3**, 1–10 (1974).
6. P. Chao, H. Ozoe, S. Churchill and N. Lior, Laminar natural convection in an inclined rectangular box with the lower surface half-heated and half-insulated, *J. Heat Transfer* **105**, 425–432 (1983).
7. G. Shiralkar and C. Tien, A numerical study of the effect of a vertical temperature difference imposed on a horizontal enclosure, *Numer. Heat Transfer* **5**, 185–197 (1982).
8. D. Poulikakos, Natural convection in a confined fluid filled space driven by a single vertical wall with warm and cold regions, *J. Heat Transfer* **107**, 867–876 (1985).
9. I. Sneddon, *Mixed Boundary Value Problems in Potential Theory*. North Holland, Amsterdam (1966).
10. J. Bassani, M. Nansteel and M. November, Adiabatic–isothermal mixed boundary conditions in heat transfer, *Int. J. Heat Mass Transfer* **30**, 903–909 (1987).
11. M. November, Natural convection in a rectangular enclosure heated and cooled on adjacent walls, M.S. Thesis, University of Pennsylvania, Philadelphia, Pennsylvania (1986).
12. W. F. Ames, *Numerical Methods for Partial Differential Equations*, 2nd Edn, p. 231. Academic Press, New York (1977).
13. G. Batchelor, Heat transfer by free convection across a closed cavity between vertical boundaries at different temperatures, *Q. Appl. Math.* **12**, 209–233 (1954).
14. M. Nansteel, S. Sadhal and P. Ayyaswamy, Discontinuous boundary temperatures in heat transfer theory, Session on Significant Questions in Buoyancy Affected Enclosure or Cavity Flows, ASME Winter Annual Meeting, December (1986).
15. M. W. Nansteel, K. Medjani and D. S. Lin, Natural convection of water near its density maximum in a rectangular enclosure: low Rayleigh number calculations, *Physics Fluids* **30**(2), 312–317 (1987).
16. G. D. Mallinson and G. de Vahl Davis, Three dimensional natural convection in a box: a numerical study, *J. Fluid Mech.* **83**, 1–31 (1977).

## CONVECTION NATURELLE DANS DES ENCEINTES RECTANGULAIRES CHAUFFEES PAR LE BAS ET REFROIDIES SUR UN COTE

**Résumé**—On étudie analytiquement et numériquement la convection naturelle permanente dans une enceinte carrée, remplie d'eau chauffée par le bas et refroidie sur un côté vertical. Des développements pour un petit nombre de Rayleigh sont obtenus à l'ordre $Ra^2$. On trouve que la première contribution à la convection thermique se produit à l'ordre $Ra^2$. Des expressions asymptotiques sont trouvées pour la température et le transfert thermique près de la singularité de flux au plancher de la cavité. Des simulations numériques par différences finies montrent que la condition étudiée (chauffage par le bas) est tout à fait distincte du cas du refroidissement par le bas et chauffage sur un côté vertical. Le transfert thermique convectif est plus significatif quand un peu moins de la miotié de la surface inférieure est chauffée.

## NATURLICHE KONVEKTION IN RECHTWINKLIGEN HOHLRÄUMEN DIE VON UNTEN BEHEIZT UND AN EINER SEITE GEKÜHLT WERDEN

**Zusammenfassung**—Die stationäre natürliche Konvektion in einem quadratischen, wassergefüllten Hohlraum, der von unten beheizt und an einer senkrechten Seite gekühlt wird, wird analytisch und numerisch untersucht. Für kleine Rayleigh-Zahlen werden Entwicklungen bis zur Ordnung $Ra^2$ angegeben. Es zeigt sich, daß der erste Beitrag zum konvektiven Wärmeübergang bei der Ordnung $Ra^2$ auftritt. Asymptotische Ausdrücke werden für die Temperaturverteilung und den Wärmeübergang in der Nähe der Strömungssingularität am Boden des Hohlraums angegeben. Numerische Simulationen mit dem Finite-Differenzen-Verfahren deuten an, daß die vorliegende Bedingung (Heizen von unten) völlig verschieden vom umgekehrten Fall (Kühlen von unten, Heizen an einer vertikalen Wand) ist. Es wird gezeigt, daß der konvektive Wärmeübergang am intensivsten ist, wenn etwas weniger als die Hälfe der unteren Fläche geheizt wird.

## ЕСТЕСТВЕННАЯ КОНВЕКЦИЯ В ПОЛОСТЯХ ПРЯМОУГОЛЬНОГО СЕЧЕНИЯ ПРИ НАГРЕВЕ СНИЗУ И ОХЛАЖДЕНИИ СБОКУ

**Аннотация**—Аналитически и численно исследована стационарная естественная конвекция воды в полости квадратного сечения, нагреваемой снизу и охлаждаемой вдоль одной вертикальной стенки. В качестве малого параметра используется число Рэлея, разложение по которому ведется с точностью до квадратичных членов. Обнаружено, что влияние конвективного теплопереноса проявляется в квадратичном приближении по числу Рэлея. Получены асимптотические выражения для температуры и теплопереноса в окрестности особой точки, находящейся на дне полости. Численное моделирование методом конечных разностей свидетельствует о том, что указанное выше условие (нагрев снизу) приводит к структуре естественной конвекции, совершенно отличной от структуры конвекции при охлаждении снизу и нагреве вдоль вертикальной стенки. Показано, что конвективный теплоперенос является наиболее интенсивным, если нагревать чуть меньше половины поверхности дна полости.